

Supporting Information

Asymmetric heterojunction between size different 2D flakes intensify the ionic diode behaviour

He Ma,^a Xiaoheng Jin,^b Yun-Zhe Du,^a Ling-Yu Dong,^a Xu Hu,^a Wen-Cui Li,^a Dongqi Wang,^a Rakesh Joshi,^b Guang-Ping Hao,^{a*} An-Hui Lu^a

a. State Key Laboratory of Fine Chemicals, Liaoning Key Laboratory for Catalytic Conversion of Carbon Resources, School of Chemical Engineering, Dalian University of Technology, Dalian 116024, P. R. China. E-mail: guangpinghao@dlut.edu.cn

b. School of Material Science and Engineering, University of New South Wales, Gate 2 High St Kensington, NSW 2052, Australia

† Electronic Supplementary Information (ESI) available. See DOI: 10.1039/x0xx00000x

Experiment

Materials and methods.

Chemicals. All chemicals were purchased and used as received without further purification unless otherwise stated. Potassium chloride (AR), and hydrogen chloride (AR) were purchased from Sinopharm Chemical Reagent Co., Ltd. Polydimethylsiloxane (PDMS) was purchased from Dow Corning.

Characterization. Powder X-ray diffraction (XRD) measurements were conducted with a PANalytical X'Pert3 powder diffractometer with Cu K α radiation ($\lambda = 1.5406 \text{ \AA}$). The X-ray photoelectron spectroscopy (XPS, ESCALAB XI+) was measured on the film surface to analyse the content of oxygen-containing functional group on GOM. Zeta potential of S-GO and L-GO colloids was measured to characterize the charge properties (Malvern Zetasizer NanoZS90). The contact angle of S-GOM and L-GOM were characterized with contact angle tester (HARKE-SPCA). The electrochemical measurements were performed using an electrochemical workstation (Ivium-n-Stat, Netherlands, 1.5 pA). The Fourier transform infrared spectroscopy (FTIR) was recorded on a Bruker 70V spectrometer to analysed the chemical composition of the S-GOM and L-GOM.

Electrical Measurement. A piece of asy-GOM (**Fig. 1e**) was put in nanofluidic device (**Fig. 1e bottom**). The effective membrane area was 0.25 cm^2 . The transmembrane current was recorded with electrochemical workstation (Ivium-n-Stat, Netherlands, 1.5 pA) through Ag/AgCl electrodes. Two Ag/AgCl electrodes were inserted into reservoirs to measure proton current through the membranes. The I-V curves of the nanofluidic devices were recorded at different HCl concentrations. The conductivity (λ) is calculated from the equation $\lambda = G(l/hw)$, where G is the measured conductance (slope of the I-V curve) and l , h and w are the length, height, and width of the channels, respectively. All the experimental measurements are conducted at the room temperature of around $25 \text{ }^\circ\text{C}$. The bulk conductivity of the HCl (**Fig.3e**) is given by:

$$c = \frac{k}{\Lambda_m}$$

which c and Λ_m are the concentration and the molar conductivity in the solution, respectively; k is the conductivity.

Effects of the temperature on conductivity. To study the temperature effect on nanofluidic ionic current, the GOM is embedded into a PDMS block, and the PDMS block is heated in water bath along with a thermometer, as shown schematically in **Fig. S13**. The ends of the membrane were exposed to 10^{-4} M HCl solution. The acid-soaking device was then immersed into water bath that was heated at a rate of $0.25 \text{ }^\circ\text{C}/\text{min}$ from $20 \text{ }^\circ\text{C}$ to $60 \text{ }^\circ\text{C}$. At regular intervals, the ionic conductance was recorded by measuring I-V curves, while the water bath temperature was monitored a thermometer. The current was recorded with electrochemical workstation (Ivium-n-Stat). Based on the measured conductance at five different temperatures, the active energy (E_a) is calculated based on the following formula:

$$\ln k = \frac{-E_a}{RT} + \ln A$$

which k is the conductivity, the R is molar gas constant, the T is the Kelvin temperature and the A is the pre-exponential factor.

Measurement of Debye length. The Debye Length (λ_D), which is the thickness of the double layer that forms at the charged surface in an electrolytic solution, is given by:

$$\lambda_D = \left(\sum_i \frac{\rho_i e^2 z_i^2}{\varepsilon \varepsilon_0 k_B T} \right)^{-1}$$

which ρ and Z are the concentration and charge of ionized species in the solution, ε is the permittivity of vacuum, ε_0 is the dielectric constant, k_B is the Boltzmann constant, and T is the temperature. The monovalent salt solution can be simplified the above equation to,

$$\lambda_D = \frac{0.304}{\sqrt{|M|}}$$

which M is the concentration of the salt solution.

Measurement of surface charge density. Based on the electric double layer (EDL) theory, the relationship between the zeta potential (ζ) and the effective charge density (σ_{eff}) can be expressed by the modified Gouy-Chapman equation,¹

$$\sigma_{eff} = \sqrt{8cN_0\varepsilon_r\varepsilon_0k_B T} \sinh\left(\frac{e\zeta}{2k_B T}\right)$$

$$\Delta\sigma = \frac{(\sigma_{S-GO} - \sigma_{L-GO})}{\sigma_{L-GO}} = \frac{\sinh\left(\frac{e\xi_{S-GO}}{2k_B T}\right) - \sinh\left(\frac{e\xi_{L-GO}}{2k_B T}\right)}{\sinh\left(\frac{e\xi_{L-GO}}{2k_B T}\right)}$$

Where the c stands for the ion concentration, N_0 is the Avogadro constant, ε_r is the relative dielectric permittivity of the solution, ε_0 is the vacuum permittivity, k_B is Boltzmann's constant, and T is the Kelvin temperature.

Synthetic procedures

Preparation of graphene oxide membranes and nanofluidic device. Graphene oxide (GO) was prepared by modified Hummer's method, and then screened by centrifugation to obtain GO with different flake size. Specifically, GO solution was centrifuged at 12000 and 6000 r.p.m to obtain large GO flakes (L-GO) and small GO flakes (S-GO), respectively. GO membranes were prepared by vacuum filtration of the separated GO dispersions. To prepare the freestanding membrane, GO solution was filtered through a nylon 6 filter membrane (50 mm diameter, 0.22 μm pore size; Jing Teng, China). The GO membrane was cut into desirable size, a 5×5 mm rectangular symmetric film, and put the GO strip into the PDMS which were carved two reservoirs to expose the end of GO membrane into the electrolyte solution.²

Preparation of asy-GOM and asy-mod-GOM. Asymmetric GO membranes are consisted of different lateral size. The asy-GOM was fabricated by stepwise filtration of L-GO solution and S-GO solution. To improve the stability, we used the KCl with varied concentration for the modification of S-GO (0.1 M) and L-GO (1 M) part.

Supporting Figures

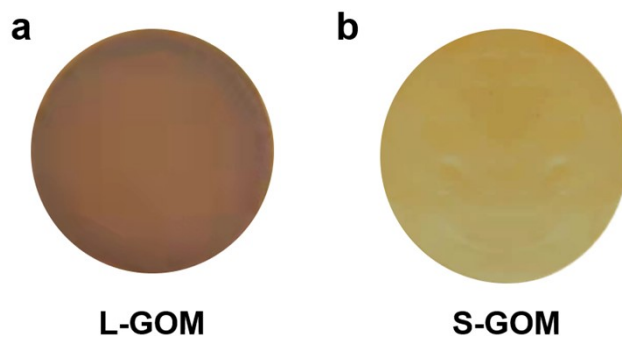


Fig. S1 Digital photos of the (a) L-GOM and (b) S-GOM.

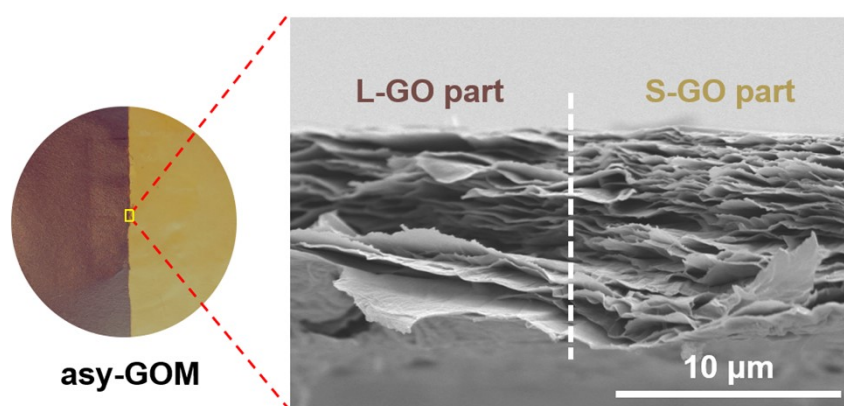


Fig. S2 SEM images of the cross section of the asy-GOM.

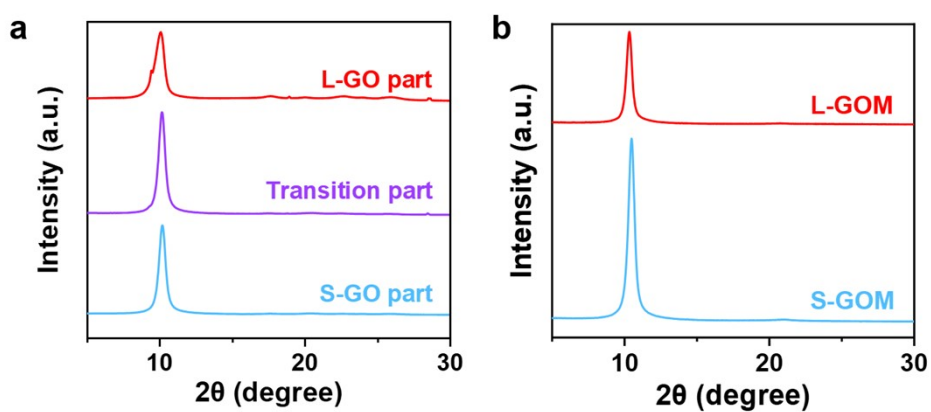


Fig. S3 XRD patterns for (a) different regions in the asy-GOM, (b) individual membrane of L-GOM and S-GOM.

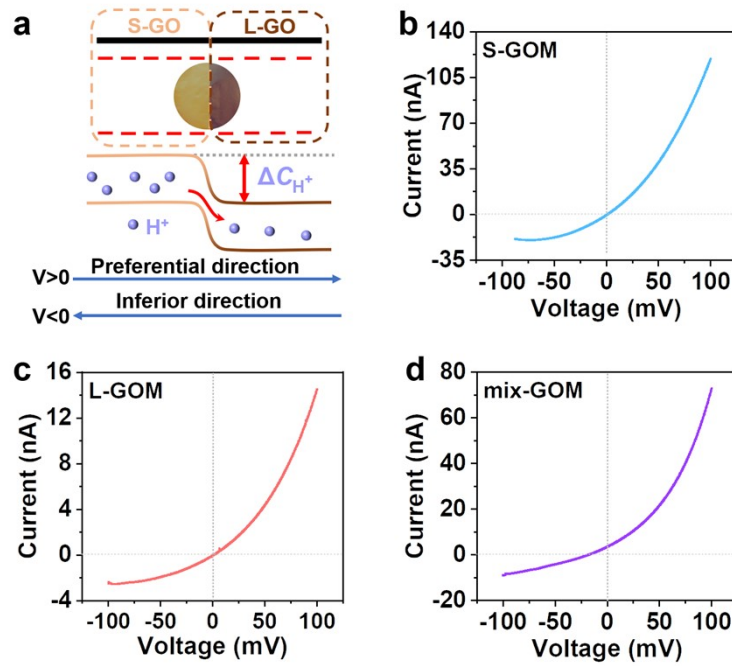


Fig. S4 (a) The schematic illustration for asymmetric proton transport through asy-GOM, typical I-V curves for (b) S-GOM, (c) L-GOM and (d) mix-GOM.

In symmetric GOM, the protons mainly transport in the nanochannel because the negatively charged GO nanosheets can attract the H^+ cations but repel the Cl^- anions. In the potential ($V_{app} < 0$), the ion channel is blocked by the accumulated proton via physical adsorption and only a low leakage current exists. When a reverse potential is applied ($V_{app} > 0$), protons are driven to approach the nanochannel and a continuous ionic current can be maintained due to the proton transport. At the asy-GOM heterojunction, the asymmetric surface charge distribution led to an intramembrane proton concentration gradient (ΔC_{H^+}), which intensified the rectification behaviour. For $V_{app} > 0$, the proton transport is from the S-GO to the L-GO, parallel to the (ΔC_{H^+}). Therefore, it becomes the preferential direction for proton transport. On the contrary, for $V_{app} < 0$, the protons migrate in the antiparallel direction to the (ΔC_{H^+}), and result in relatively low proton conductance.

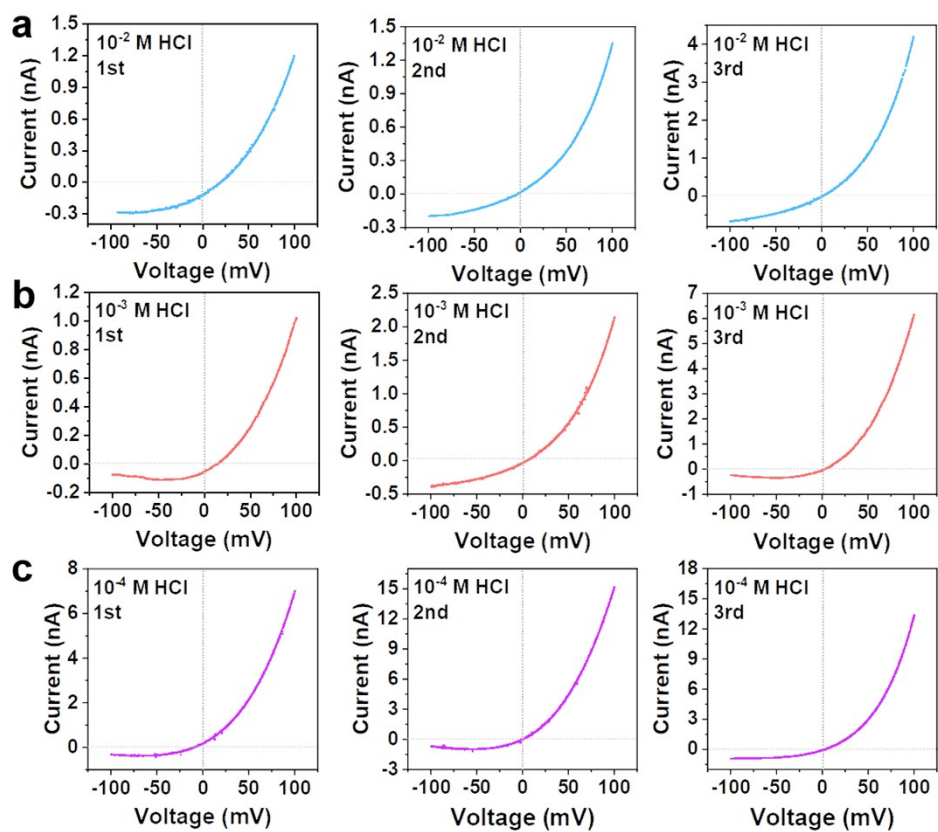


Fig. S5 The original I-V data for asy-GOM in HCl electrolyte with concentration of 10^{-2} M (a), 10^{-3} M (b) and 10^{-4} M (c).

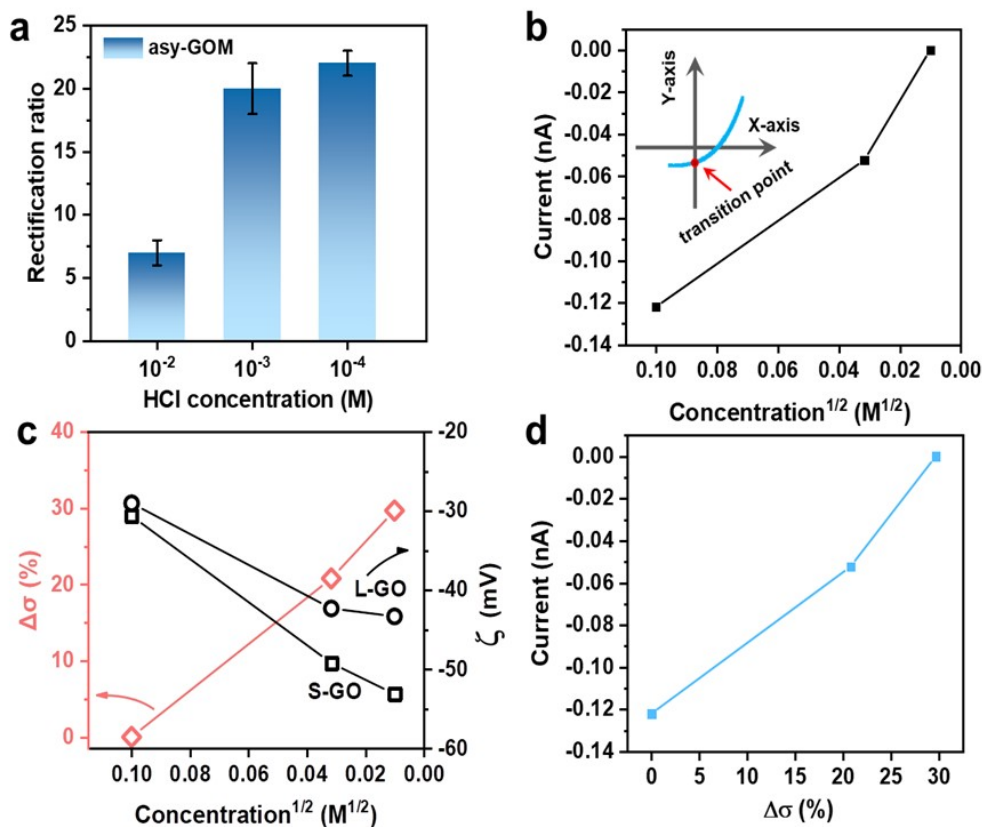


Fig. S6 (a) The rectification ratio for asy-GOM with different concentration. (b) The correlation between the proton concentration and the current at transition points. Inset: Transition point is defined as the shifting from the origin point (0, 0) at the condition of no bias voltage applied. (c) The proton concentrations dependent Zeta potential (ζ) as well as the difference of surface charge density ($\Delta\sigma$). (d) The correlation of $\Delta\sigma$ and the current at transition points.

As discussed in the mentioned finding,³ the cross-point potential indicates the transition between the high and low conductivity states. In nature, it is analogous to the isosbestic point in spectroscopic measurements. Accordingly, in this work, the transition point is defined as the shifting from the origin point (0, 0) at the condition of no bias voltage applied (**Fig. S6b inset**).

The nonzero cross-point potential is found dependent on the proton concentrations, or say pH. We have investigated the proton concentration effects on the Zeta potential (ζ) as well as the surface charge differences, which further affect the current of transition points. For instance, the current at transition points was found decreased as increasing proton concentrations (**Fig.S6b**), which is consistent with the previous finding.³ This trend is consistent to the ICR behavior at varied proton concentrations. By analyzing the Zeta potential (ζ), we found the shifting from the origin is relevant to the surface charge gradient (**Fig.S6c,d**).

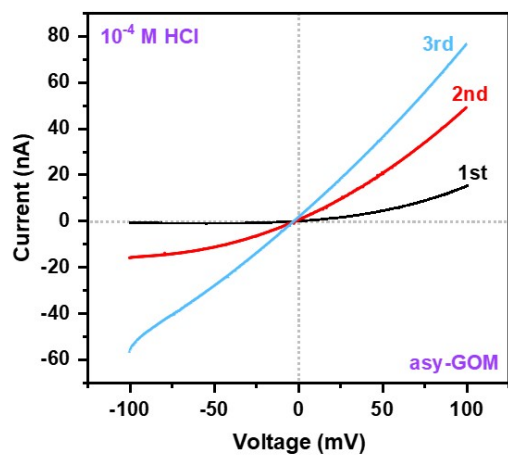


Fig. S7 The multiple I-V scans for asy-GOM in 10^{-4} M HCl.

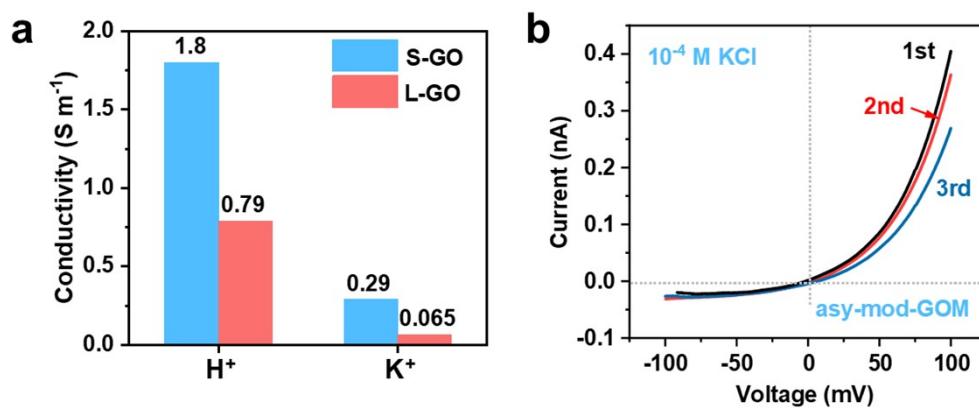


Fig. S8 (a) The comparison ionic conductivity of K^+ and H^+ in 10^{-4} M, (b) the multiple I-V curves for asy-mod-GOM in 10^{-4} M KCl.

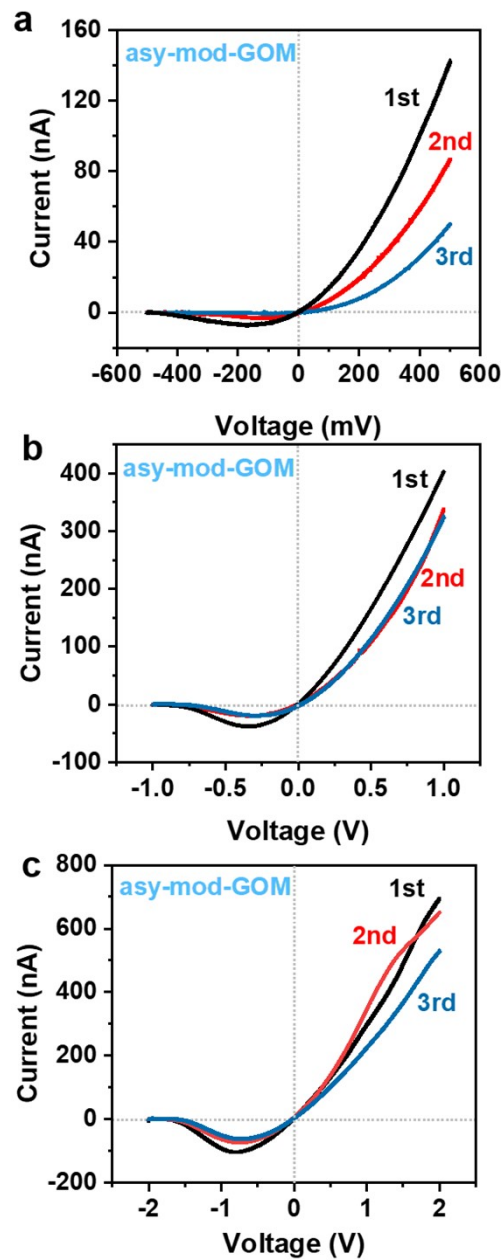


Fig. S9 The multiple I-V curves for asy-mod-GOM in 10^{-4} M HCl with the scan range of ± 0.5 V (a), ± 1 V (b) and ± 2 V (c)

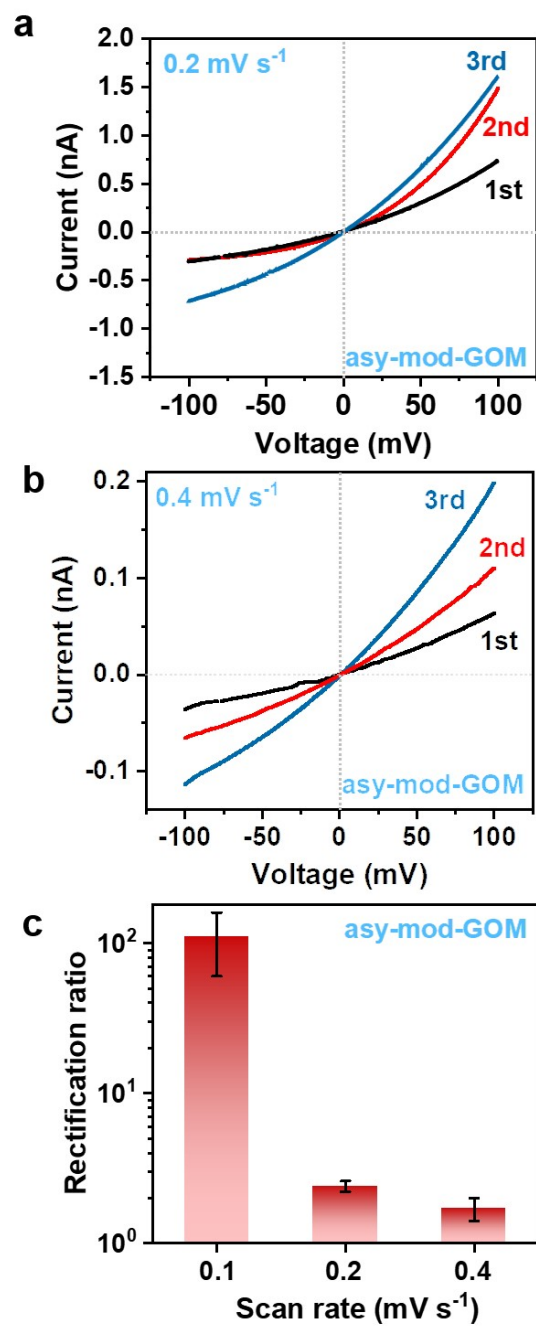


Fig. S10 (a, b) The multiple I-V curves for asy-mod-GOM in 10^{-4} M HCl with the scan rate of 0.2 mV s^{-1} and 0.4 mV s^{-1} and their corresponding rectification ratio (c).

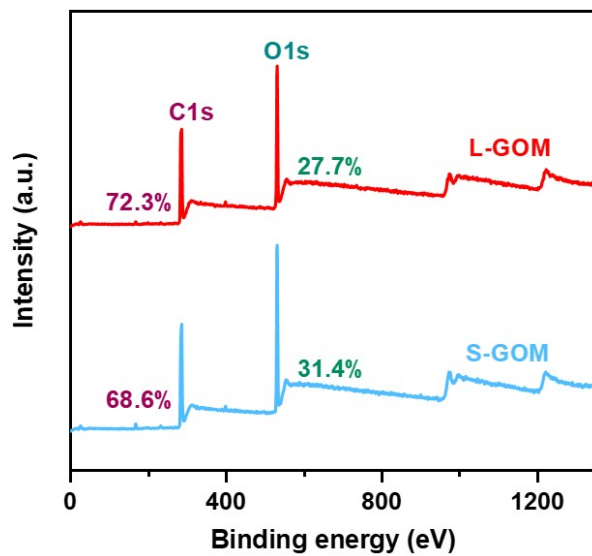


Fig. S11 The XPS survey spectra for S-GOM and L-GOM.

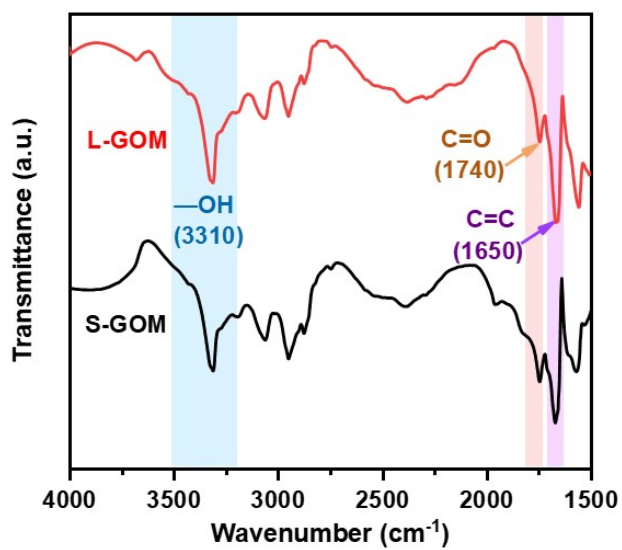


Fig. S12 The FTIR spectra for S-GOM and L-GOM.

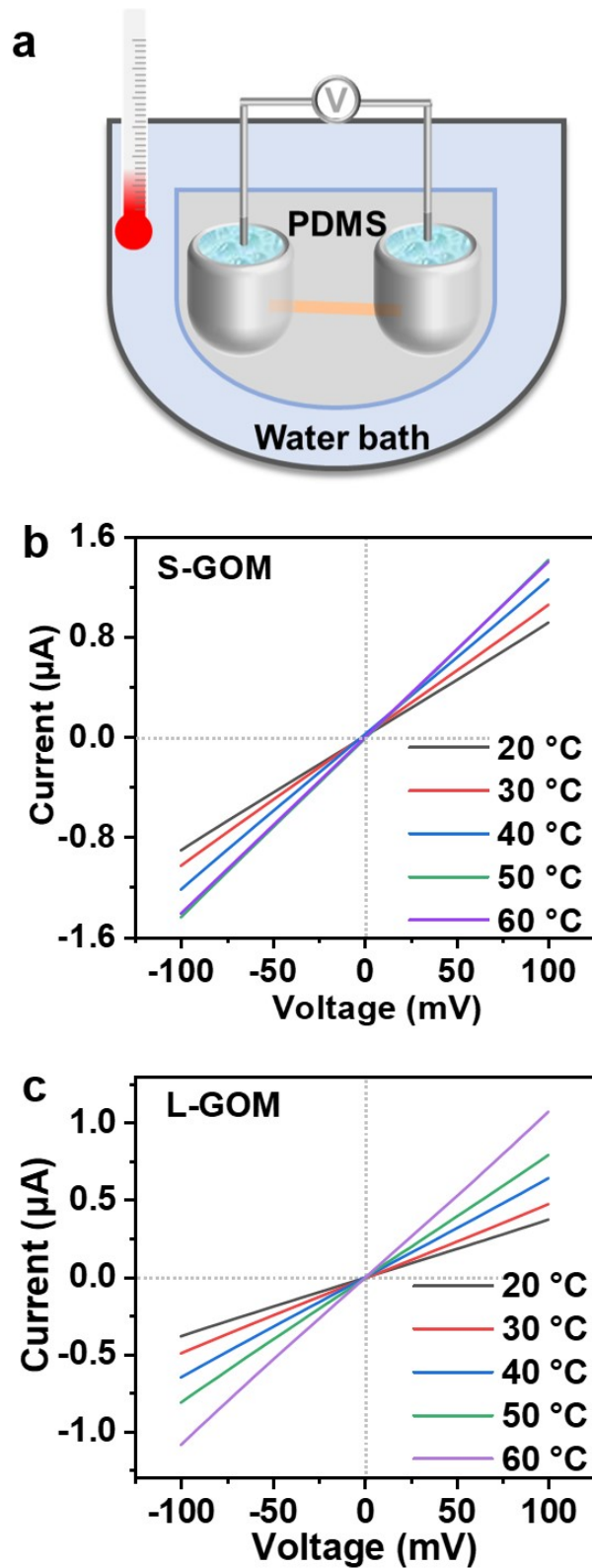


Fig. S13 (a) The test sketch for the proton conductivity at varied temperatures, (b,c) typical I-V curves for S-GOM and L-GOM at different temperatures.

Supporting Tables

Table S1. The comparison of rectification performances in the KCl and HCl electrolytes.

ID	Scan rate /potential range	Electrolyte concentration	Rectification ratio
asy-mod-GOM	0.1 mV s ⁻¹ /±0.1 V	10 ⁻⁴ M KCl	23 ± 0.5
	0.2 mV s ⁻¹ /±0.1 V	10 ⁻⁴ M HCl	2.4 ± 0.2
	0.4 mV s ⁻¹ /±0.1 V	10 ⁻⁴ M HCl	1.7 ± 0.3
	0.1 mV s ⁻¹ /±0.5 V	10 ⁻⁴ M HCl	630 ± 219
	0.1 mV s ⁻¹ /±1 V	10 ⁻⁴ M HCl	1404 ± 347
	0.1 mV s ⁻¹ /±2 V	10 ⁻⁴ M HCl	29113 ± 14177

Reference

- 1 Z. Ge and Y. Wang, *J. Phys. Chem. B*, 2017, 121, 3394–3402.
- 2 K. Raidongia and J. Huang, *J. Am. Chem. Soc.*, 2012, 134, 16528–16531.
- 3 D. Wang, M. Kvetny, J. Liu, W. Brown, Y. Li, and G. Wang, *J. Am. Chem. Soc.*, 2012, 134, 3651–3654.